Stable Lateral Motion Control with Motor-controlled Wheels

Shin-ichiro Sakai Yoichi Hori

Abstract

The actuator of electric vehicle is electric motor, which has excellent performance for motion control applications. Its torque response is quite fast and accurate, and it can be distributed for several wheels. This paper proposes stable lateral motion control method of EV, based on these advantages. With fast torque response, linear feedback controller can be applied. The anti-slip control can be achieved with feedback of wheel velocity, which is easily measured. If every wheel has driving motor, this anti-slip controller can be applied for every wheel. These "motor-controlled" wheels affect the vehicle lateral motion on slippery road. Our simulations and experimental results both indicate that vehicle with "motor-controlled" wheels have stabilized lateral dynamics. These wheel feedback controllers are the independent ones, therefore, can be minor loops of another controller. In the latter part of this paper, the effects of these minor loops are studied, when combined with lateral motion controller. The simulation results show that "motor-controlled" wheels improve the stability of direct yaw-moment control (DYC), which is a typical lateral motion controller. It suggests an advanced control system of total vehicle motion of EV, which is an integration of longitudinal and lateral control.

keywords: traction control, control system, braking, safety.

1. Introduction

The actuators for vehicle motion control will be, or actually is, improved. For example, some researches seem to intend to develop fast and linear braking actuators. The driving and braking actuator of electric vehicle (EV) is an electric motor, which is a typical and ideal example of such advanced actuators. EV itself is now developed significantly, as well known it is. Hybrid EVs (HEVs) like Toyota Prius seem to have succeeded commercially, and fuel cell EVs (FCEVs) are believed to be major vehicles in the next decade. Thus, studies on motion control of EV are important, 1) to know the possibility of advanced actuators for conventional vehicle, and 2) to discuss on the novel and basic strategies for EV's motion control.

From the viewpoint of electrical and control engineering, EVs have evident advantages over internal combustion engine vehicles (ICVs). These advantages can be summarized as:

1. ***Torque generation of electric motor is very quick and accurate, for both accelerating and decelerating.***

   This should be the essential advantage. ABS (antilock brake system) and TCS (traction control system) should be integrated into "total TCS", since a motor can both accelerate or decelerate the wheel. Its performance should be advanced one, if we can fully utilize the fast torque response of electric motor [1].

2. ***Motor can be attached to each wheel.***

   With small motors like in-wheel motors [2], even the anti-directional torque generation is possible on left and right wheels. In automobile engineering, such approach is known as DYC (direct yaw moment control) [3] [4]. Distributed motor will possibly enhance its performance.

3. ***Motor torque is easily comprehensible.***

   There exists little uncertainty in driving or braking torque generated by motor, compared to that of combustion engine or hydraulic brake. Therefore, simple "driving force observer" can achieve a real-time observation of driving/braking force between the tire and road surface [5]. This second advantage will contribute a great deal to several applications like road condition estimation.

Definitely, these suggest the novel approach for vehicle motion control. It is also available with conventional vehicles, if fast and linear actuator can be applied for driving and braking. Here we treat EV as an example of such advanced vehicles.
Then, how should these advantages be utilized? Minor feedback with fast torque response is the basic strategy of this paper. This fast feedback approach is quite general in motion control engineering, such as robotics. It was difficult in conventional vehicle, however, is available with EV. One typical example of such approach is the wheel feedback controller for anti-skid control. This is a linear feedback controller of wheel velocity, designed to prevent its sudden change. This anti-skid effect is clearly demonstrated with experiments in this paper.
This proposed controller is designed to nominalize the wheel dynamics, to enhance the robustness against the sudden road condition changes. It can be a minor loop of vehicle motion controller, such as DYC. If each driven wheel is actuated by electric motor, the proposed controller can be applied for every driven wheel. This "controlled wheel" is robust for road condition, and it enhances the stability of total control system. In the latter parts of paper, this idea is studied with both simulations and experiments.
"UOT Electric March II" was projected to carry out experimental studies on these lateral dynamics of EV. It is "four-wheel motored EV": every wheel has its own driving motor. We have already designed and completed this EV. Before the academic discussions, this EV is introduced in the next section.

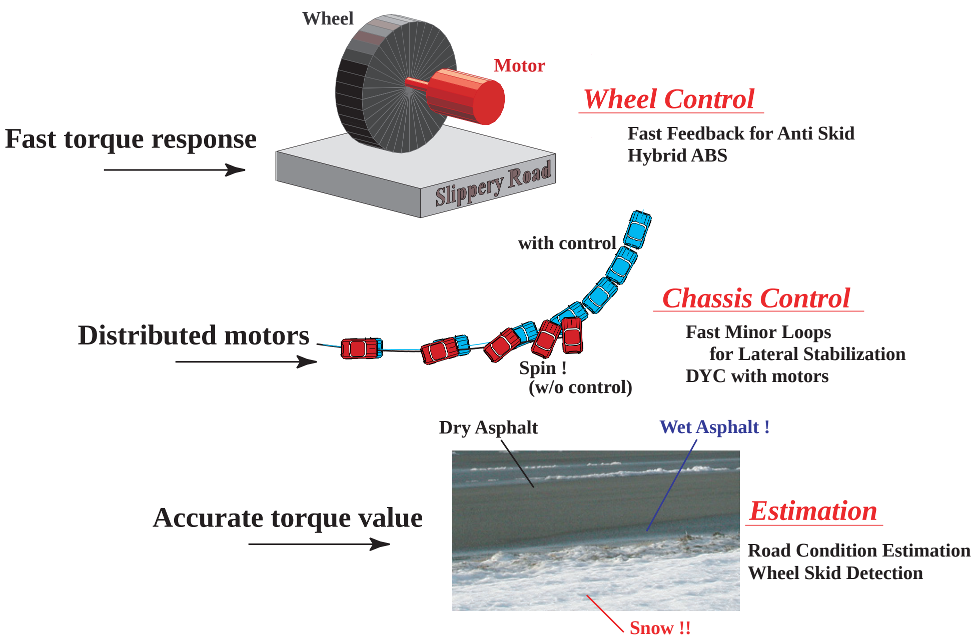

Figure 1: EV's three essential advantages in motion control issues.

2. "UOT Electric March II", Novel Four Wheel Motored EV

In 1997, we constructed "UOT Electric March I", which is our first EV for motion control experiments. This vehicle was very simple: driven with only one DC motor, and no regenerative braking system. Several studies on longitudinal motion control were carried out with this EV [1].
"UOT Electric March II" is our novel EV. It was projected in 1998, and completed in 2001 [6]. This EV can be characterized by its original motor configuration: 4 independent driving motors

(Fig. 2). Each wheel has driving in-wheel motor (Fig. 3), therefore, every driven wheel can be independently controlled. Regenerative braking is also available with these motors. We ourselves designed and built up this vehicle, based on the conventional ICV "Nissan March".
The specification of this EV focuses on the motion control experiments. It has adequate devices for experiments: on-board PCs and several sensors like fiber-optic gyro and accelerometer. Motion controller on the PC outputs the torque commands, and inverter units generate the torques of these values. Table 1 summarizes the key specifications of "UOT Electric March II". Every construction process was proceeded by authors(Fig. 4), and shakedown was carrid out on Jan., 2001(Fig. 5).

Table 1: Spec of "UOT Electric March II"

Drivetrain	**4 PM Motors**
Max. Power(20 sec.)	36 [kW] (48.3[HP])*
Max. Torque	77* [Nm]
Gear Ratio	5.0
Battery	**Lead Acid**
Weight	14.0 [kg](for 1 unit)
Total Voltage	228 [V] (with 19 units)
Base Chassis	**Nissan March K11**
Wheel Base	2360 [mm]
Wheel Tread F/R	1365/1325 [mm]
Total Weight	1400 [kg]
Wheel Radius	0.28 [m]
Controller	
CPU	MMX Pentium 233[MHz]
Control Period	1 [ms]
Rotary Encoder	3600 [ppr]***
Gyro Sensor	Fiber Optical Type

* ... for only one motor.

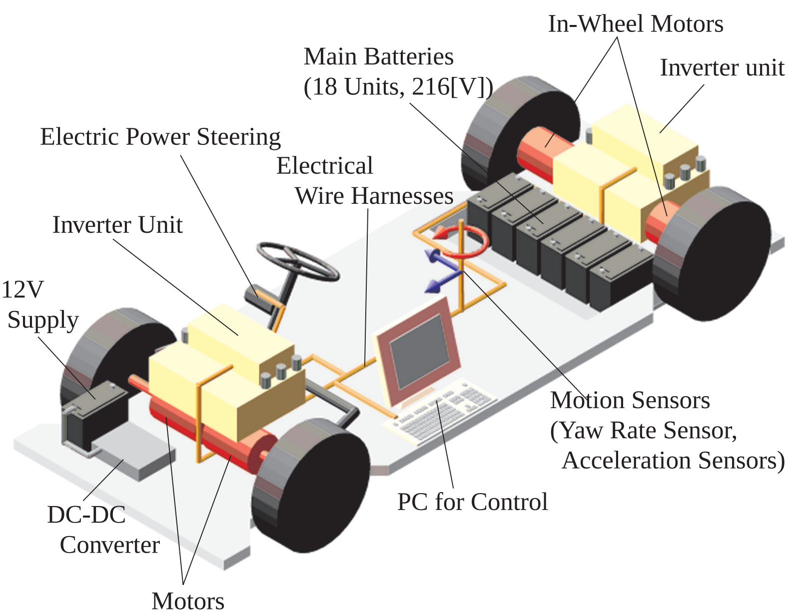

Figure 2: Design concept of "UOT Electric March II"

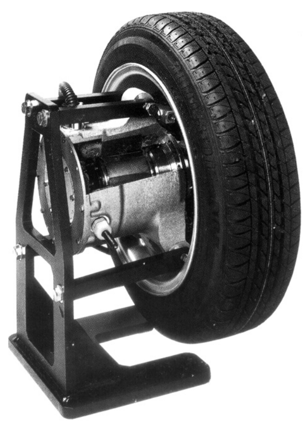

Figure 3: Photo of in-wheel motor.

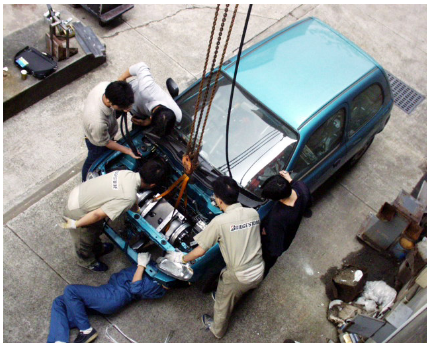

Figure 4: Construction “UOT Electric March II” by authors.

Figure 5: “UOT Electric March II” running at 100 [km/h].

3. Wheel Velocity Feedback For Slip Prevention

In this section, the wheel velocity controller for skid prevention is discussed. The starting point of this idea is to utilize the knowledge on motion control, which is based on the motor control. In general, the feedback controller can change the dynamics of plant, or we can re-design the plant dynamics. For example, the plant can be insensitive against disturbance if appropriate feedback controller is applied. Such feedback controller requires fast response of actuator, and it is available in EVs. In this section, wheel velocity feedback controller is designed to utilize fast torque response.

3.1. Basic Slip phenomena and linear slip model

With simple one wheel model, the motion equations of wheel and chassis are,

$$M_w \frac{dV_w}{dt} = F_m - F_d(\lambda), \quad (1)$$

$$M \frac{dV}{dt} = F_d(\lambda), \quad (2)$$

where V and V_w are the vehicle chassis velocity and wheel velocity, respectively. Note that $V_w = r\omega$, where r, ω are the wheel radius and wheel rotating velocity, respectively. λ denotes slip ratio, and s is a laplace operator in this paper. Air resistance on chassis and rotating resistance on wheel are both neglected. M and M_w are the vehicle weight and the mass equivalent value of wheel inertia, respectively. F_m is the force equivalent value of accelerating/decelerating torque, generated by engine, hydraulic brake system or motor. F_d is the driving/braking force between the wheel and the road surface [1].

For the controller design process, linear skid model is derived from (1), (2) and $F_d(\lambda)$. Nonlinearity exists in the definition of λ or $F_d(\lambda)$, therefore, perturbation equations such as

$$\Delta F_d = N\Delta\mu = Na\Delta\lambda \tag{3}$$

$$= -\frac{1}{V_{w0}}\Delta V + \frac{V_0}{V_{w0}^2}\Delta V_w \tag{4}$$

are used here. The parameter a is a local gradient of $\mu - \lambda$ curve,

$$a = \left.\frac{\partial\mu}{\partial\lambda}\right|_{(V_0,V_{w0})}, \tag{5}$$

where V_{w0} and V_0 are the wheel velocity and chassis velocity at the operational point, respectively. With (1), (2) and (4), the transfer function from motor torque F_m to wheel velocity V_w is

$$P(s) = \frac{\Delta V_w}{\Delta F_m} = \frac{1}{(M_w + M(1-\lambda_0))s}\frac{\tau_w s + 1}{\tau_a s + 1}, \tag{6}$$

where

$$\tau_a = \frac{M_w V_{w0}}{aN}\frac{M}{M(1-\lambda_0)+M_w}, \quad \tau_w = \frac{M V_{w0}}{aN}, \tag{7}$$

and λ_0 is the value at the operational point (V_0, V_{w0}). The most simple models of wheel dynamics can be derived from (6)-(7), as

$$P_{\text{adh}}(s) = \frac{1}{M+M_w}\frac{1}{s}, \quad P_{\text{skid}}(s) = \frac{1}{M_w}\frac{1}{s}. \tag{8}$$

where $P_{\text{adh}}(s)$ and $P_{\text{skid}}(s)$ denotes the dynamics of adhesive wheel and completely skidding wheel, respectively.

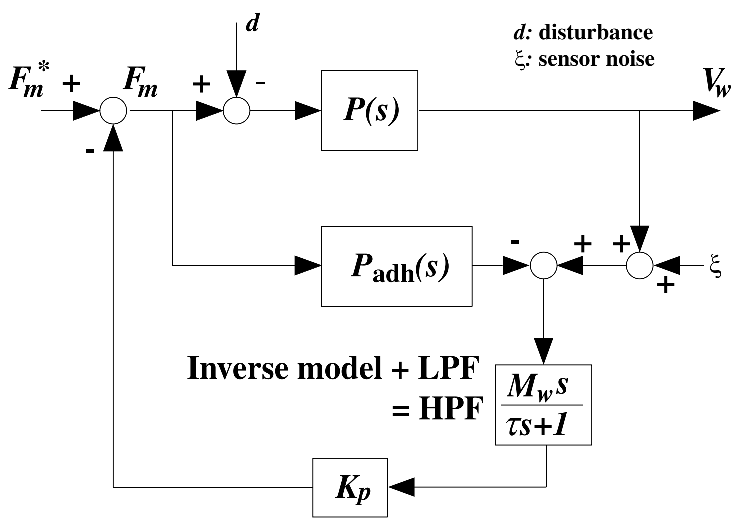

Figure 6: Proposed feedback controller.

3.2. Controller design for anti-skid

Eq. 8 indicates that wheel skidding or wheel lock can be expressed as the sudden change of wheel inertia. Based on this viewpoint, a feedback controller can be designed as Fig. 6 [1]. This controller can suppress sudden drop of wheel inertia as shown in Fig. 7.

[1] $\mu = F_d/N$, where N is the normal force on the wheel.

Fig. 7 is the bode diagram of V_w/F_m^*. Upper graph plots V_w/F_m^* for wheel without controller, i.e., plots $P_{\rm adh}(s)$ and $P_{\rm skid}(s)$. If the controller of Fig. 6 is applied, these transfer functions are changed into the ones in the lower graph. These figures clearly indicate that the dynamics of skidding wheel comes to be almost same as that of adhesive wheel, the "heavy" wheel. Thus the wheel with proposed controller is insensitive for slip phenomena.

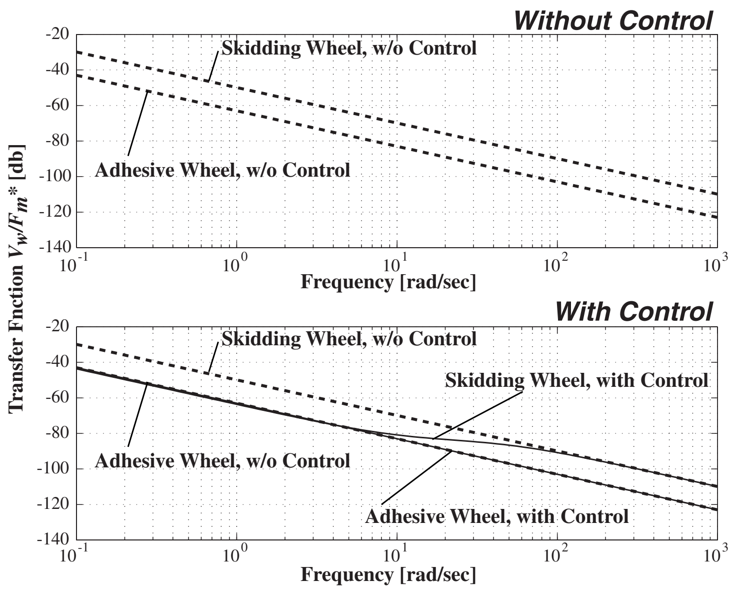

Figure 7: Bode diagram of V_w/F_m^*. $K_p = K_p{}^* = \frac{M+M_w}{M_w}$. $\tau = 0.1[sec]$.

3.3. Experiments of wheel velocity feedback

Experiments were carried out to confirm the proposed method, using "UOT Electric March-I". To examine the effect of wheel velocity control for skid avoidance, slippery low μ road is required. We put the aluminum plate with a length of 14[m] on the asphalt, and spread water on these plates. The peak μ of this test road is about 0.5. This value was estimated based on other experimental results.

Fig. 8 shows the time responses of slip ratio. In these experiments, vehicle accelerated on the slippery test road, with lineally increasing motor torque. Without control, the slip ratio rapidly increases. On the contrary, the increase of slip ratio is relatively slow with proposed controller. As mentioned above, the wheel equivalent inertia during the wheel skidding comes to be "heavy" with wheel velocity control, thus the rapid increase of slip ratio can be suppressed.

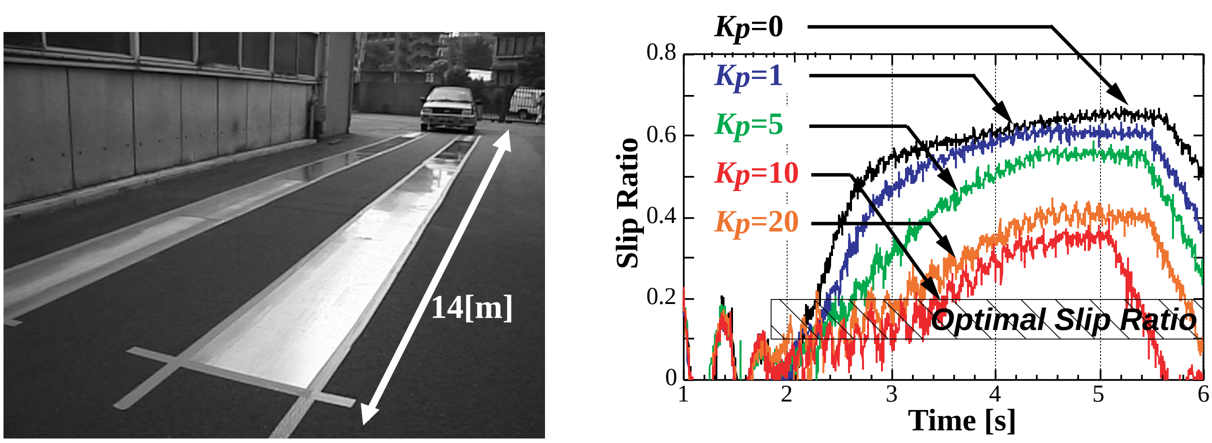

Figure 8: Effect of wheel velocity control for skid prevention with τ=0.1[s] (Experimental results.) K_p^* is 4.52 for this vehicle.

4. Lateral Motion Stabilization with Motor Control

4.1. Concept and Simulation Studies

In the previous section, wheel velocity feedback method was discussed. With this method, wheel equivalently has heavy inertia during slip. This suppresses the rapid increase of slip ratio. Then, what will happen if we apply such feedback loop for every wheel of turning vehicle on slippery road? (Fig. 9)

As commonly known, the vehicle lateral motion can be sometimes unstable. This instability occurs in such situation as rapid braking during turning, especially with slippery road condition with snowy or rainy weather. Here we assume that one small motor is attached on every wheel of target EV. In-wheel motor is one typical example. With such motors, the wheel velocities can be controlled independently. Our simulation results (Fig. 10) show that this minor loops can enhance the vehicle's lateral stability [7].

In these simulations, chassis's 3-DOF nonlinear motion, four wheel's rotation and dynamic load distribution are calculated. The vehicle starts running on the slippery road ($\mu_{\text{peak}} = 0.5$), turning left with steering angle $\delta_f = 3$ [deg]. Then at 5.0 [sec], the driver inputs rapid braking torque $F_m = -1100$[N] on each wheel. This torque exceeds the adhesion performance. Therefore, wheel skid occurs and the chassis starts spin motion, although the driver stops braking at 9.0 [s]. This wheel skidding is serious at rear-left wheel especially, since the center-of-gravity is shifted and the load distribution varied.

On the contrary, if the wheel velocity controller is applied independently for each wheel, such dangerous spin motion can be prevented (Fig. 10). The rear-inside wheel's torque is most reduced automatically. Note that this method uses only wheel velocities as feedback signals, therefore, differs considerably from conventional methods like DYC [3] [8]. The autonomous stabilization of each wheel, which is achieved with wheel velocity feedback, enhances the stability of vehicle lateral motion on slippery road. This effect is demonstrated in the next subsection.

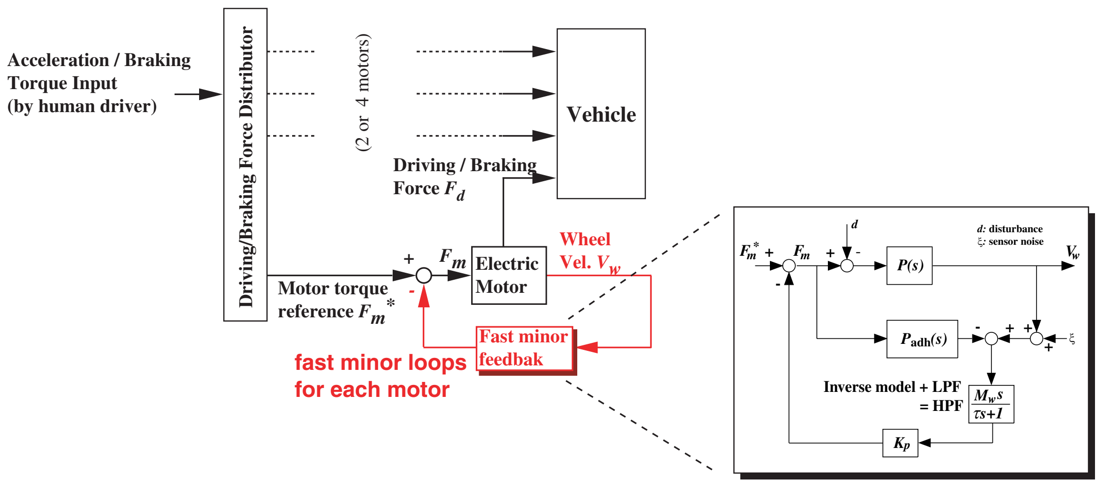

Figure 9: Vehicle with "motor-controlled" wheels.

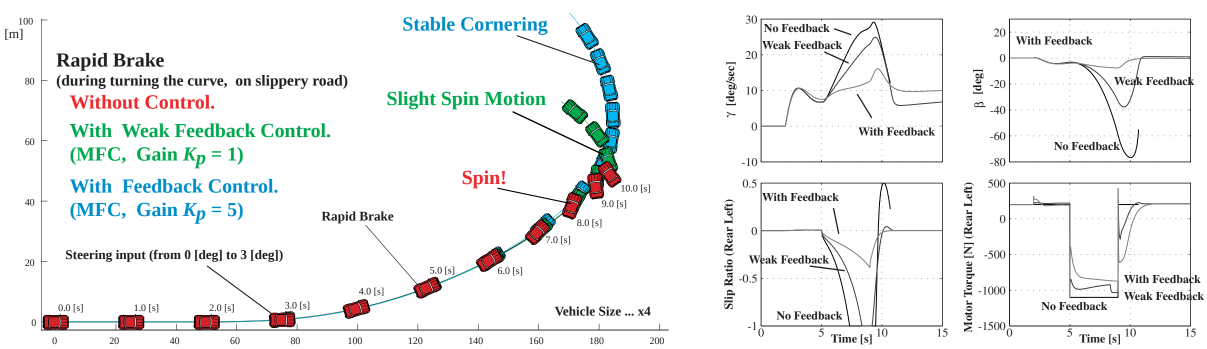

Figure 10: Stabilizing effect with "controlled four wheels" is simulated [7].

4.2. Basic Experimental Results with "UOT Electric March II"

Experiments of this method were carried out using "UOT Electric March II", with slippery test road so-called skid pad (Fig. 11). At first, it was making steady turning in the clockwise direction. Turning radius and chassis velocity were about 25-30 [m] and 40[km/h], respectively. These values were closed to the unstable region. At 0 [s], acceleration torque of 1000 [N] was applied for rear two motors. Without any feedback control, this excessive acceleration causes the unstable vehicle motion. The black line in Fig. 12 shows this unstable vehicle motion. The rear-right or rear-inside wheel started skidding seriously. Then yaw rate γ unstably grew. It indicates the spin motion. Vehicle was completely out of control, and at 2.5[sec], experiment was terminated for safety reasons.

On the contrary, such dangerous motion could be prevented with minor feedback of wheel velocity. The gray line in Fig. 12 shows this effect clearly. Note that controllers on rear-left and rear-right wheels are the same and independent ones. Each controller only requires the value of each wheel's velocity, thus it is not "connected" with each other in any meanings. Consequently, it can be said that autonomous stabilization of each driven wheel was achieved, and it enhanced the vehicle lateral stability. This indicates the validity of simulations in the previous section.

One of the remaining problems is the high frequency oscillation induced at the rear wheels. We suppose that it depends on the design of controller. The cut-off frequency τ in the proposed controller (Fig. 6) may have important influence on this oscillation, however, such discussions must wait for the next experiments.

Figure 11: Photo of turning experiments with 4W-motored EV "UOT Electric March II"

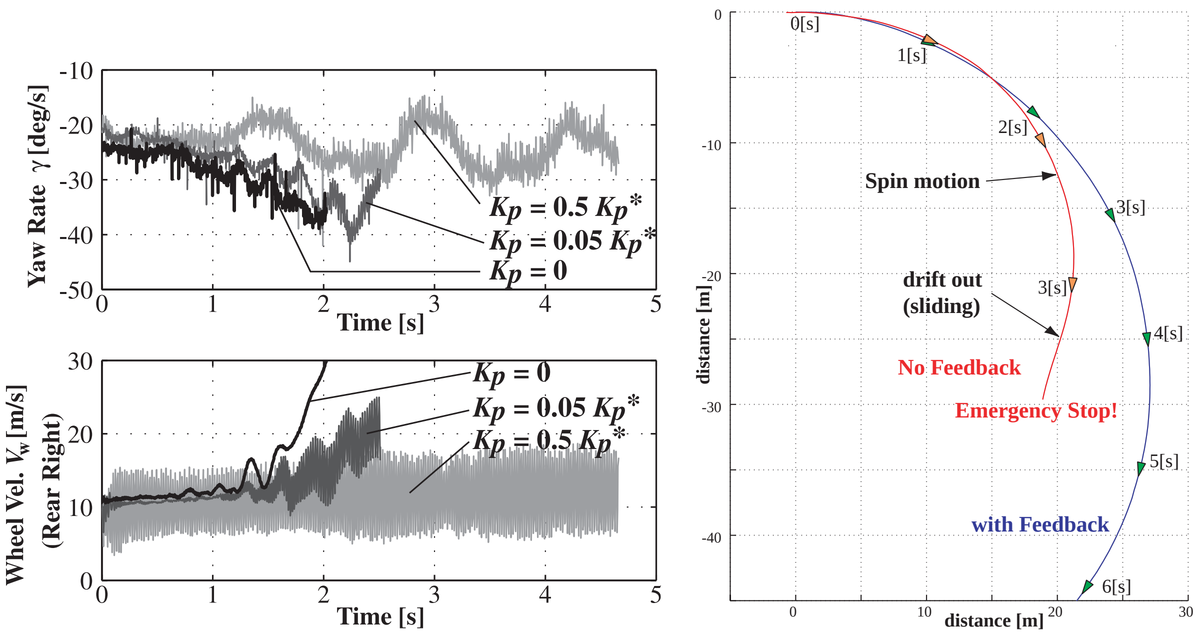

Figure 12: Comparison of experiment results: (a) without feedback controller, (b) with weak feedback controller, (c) and adequate feedback controller. K_p^* is 45.2 for this vehicle. τ in the controller was 0.1 [s]. Left: measured yaw rate and rear-inside wheel velocity. Right: measured vehicle trajectory in the experiments.

5. Stable Lateral Motion Control with Motor-controlled Wheels

The previous sections discusses on the lateral stability affected by wheel feedback control(Fig. 10). As mentioned, such feedback loop can be a minor loop controller of another major controller. For vehicle control application, chassis controller is a tipical example of such major controller. This section shows that if each wheel is "motor controlled" one, as figured in Fig.13, then the chassis controller's stability is enhanced without complicated method like β estimation [9].

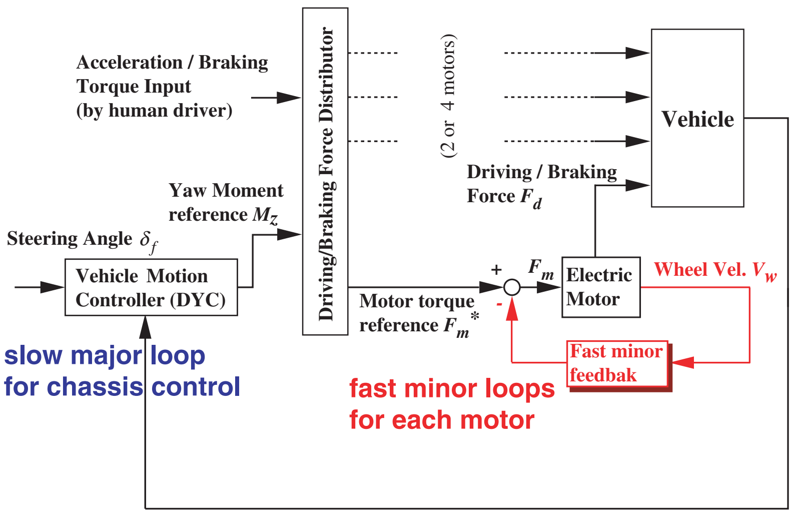

Figure 13: The block diagram of DYC + wheel velocity feedback.

5.1. Chassis controller (DYC) design

To control the vehicle lateral motion, several types of controller have been proposed. DYC [3] [8] is one general example of such chassis controllers. This paper uses DYC as chassis controller or major control loop in the following discussions. Note that the choice of chassis controller is not a point here. The main interest of this section is the effects of "motor controlled" wheel.
Basically, DYC controls chassis's yaw rate with gyro sensor. The control output of DYC is yaw moment, generated with torque difference between left and right wheels. There exists several types of DYC, however, here we select simple design based on linear bicycle model. The designed DYC controller $C(s)$ regulates the error yaw rate $\Delta\gamma$ with yaw moment M,

$$\begin{aligned} M &= C(s)\Delta\gamma, \quad C(s) = \frac{90354s^2 + 64710s + 13400}{s^2 + 11.06s + 30.34}, \\ \Delta\gamma &= \gamma^* - \gamma, \quad \gamma^* = \frac{K(V)}{0.3s+1}\delta_f, \end{aligned} \tag{9}$$

where δ_f is the front steering angle. This controller has "reference" yaw rate model, and yaw moment M is generated to make yaw rate γ follow this reference model. The effect of such DYC controller is, generally,

1. to nominalize yaw dynamics,
2. and to reject disturbance yaw moment.

Note that yaw dynamics changes with several reasons, if no controller is applied. For example, higher velocity increases transfer lag time from steering angle to yaw rate γ. It causes uncomfortable swing motion of chassis during lane-change on a highway. An example of disturbance yaw moment is a sudden gust of wind. DYC can compensate these dynamics change or disturbance.

On the other hands, the DYC controller doesn't have an effect of yaw stabilization. It cannot prevent chassis spin or skid on snowy road. It only controls the yaw rate, however, the important information on yaw stability is chassis slip angle β. Therefore, β-based controllers are proposed to stabilize chassis lateral motion [9]. One problem of this approach is that on-board measurement of β is difficult. Thus in vehicle engineering, complicated β estimation methods are eagerly studied [9].

5.2. DYC + wheel feedback controller

Based on the previous discussions, this paper proposes another approach for lateral motion stabilization. Without complicated β estimator, we simply applied wheel feedback controller for each wheel. Fig. 13 shows the block diagram of proposed method. As this figure shows, DYC in this proposed method has minor loop controllers of Fig. 6. DYC's output is yaw moment M, and it is distributed to each wheel's driving or braking torques. These torques are affected by minor controllers of Fig. 6, when wheel slip or wheel skid occurs.

Fig. 14 and 15 are simulations results to discuss on this method. In these simulations, driver applies 3 [deg] to front steering angle at 3 [sec]. At 5[sec], the driver suddenly brakes the vehicle with braking force of 1100[N], and it is applied until 9[sec]. Without control, the yaw rate response is disturbed with this sudden braking force, as shown in Fig. 14 with gray dotted line. DYC can nominalize the yaw dynamics, and then yaw rate γ follows its nominal model γ^* as plotted with black lines. On high-μ road (Fig.14) wheel feedback controller doesn't work, since no wheel skid is occurred in each case (black solid line).

On the other hand, this controller has strong effect for a vehicle on low μ road. DYC improves the yaw rate response, however, DYC itself cannot stabilize the vehicle lateral motion. The black dotted line in Fig. 15 shows this with dangerous β growth (spin motion). However, if DYC is applied with wheel feedback controller, the stability is improved. The black solid line is the response of this controller. In this case, the feedback loop of each wheel affects the lateral dynamics, and in results, unstable spin motion could be avoided. Fig.16 compare "DYC only" case and "DYC + wheel feedback controller" case with vehicle trajectories. These figures show the effects of proposed method clearly. Yaw rate response is improved by DYC, and the stability is enhanced by minor feedback of each wheel. Such feedback-based approach should be one of significant advantages of EV.

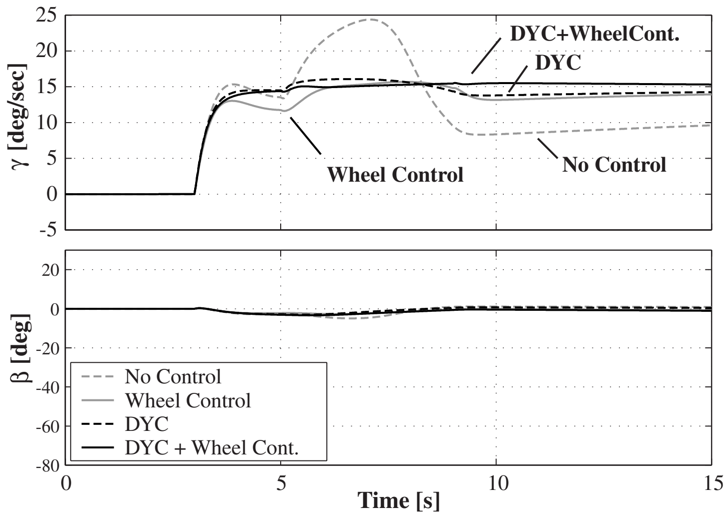

Figure 14: Vehicle Motion on $\mu = 1.0$ road (simulations).

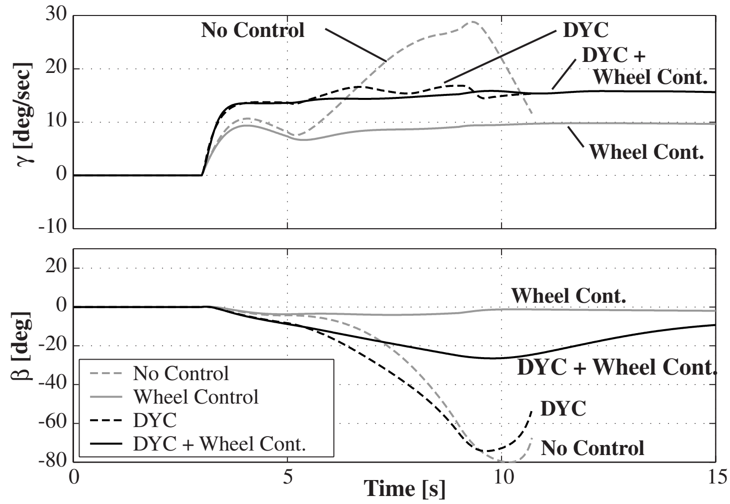

Figure 15: Vehicle Motion on $\mu = 0.5$ road (simulations).

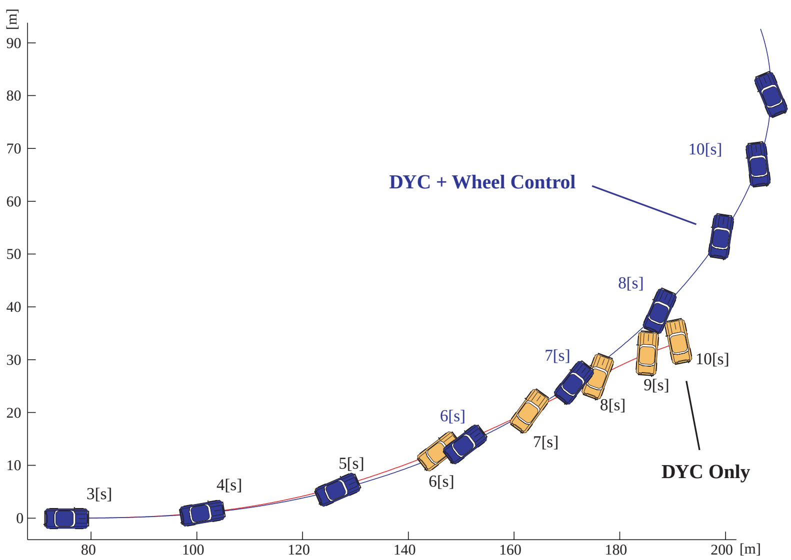

Figure 16: Vehicle Motion on $\mu = 0.5$ road (simulations).

6. Conclusion

Novel approach for vehicle motion control with fast and linear actuator is introduced. EV is one of the typical vehicle with ideal actuator, thus we discussed with experimental results with our four wheel motored EV. The advantages can be categorized into: 1) fast feedback approach for wheel skid prevention, 2) lateral stability enhancement with four motors and minor feedback loops, and 3) road condition estimation with accurate motor torque value. To study on these advantages with experiments, "UOT Electric March II" was developed. This four-wheel motored EV was completed in the spring of 2001, and will play an important roll in the coming vehicle control studies.

One of our major interests is the relation between each wheel's dynamics and chassis lateral dynamics. The experiments with "UOT Electric March II" showed that, minor loops constructed in driving wheels, or motored wheels, can stabilize the chassis lateral motion autonomously. This controller is effective even if it is combined with other chassis controller. Simulation results showed that if minor control loops are applied to driven wheels, it enhances DYC's lateral stability. Total chassis control system such as Fig. 13 will be demonstrated with "UOT Electric March II", however, still remains for future works.

References

[1] Y. Hori, Y. Toyoda, and Y. Tsuruoka, "Traction control of electric vehicle: Basic experimental results using the test EV "UOT Electric March"," *IEEE Trans. Ind. Applicat.*, vol. 34, no. 5, pp. 1131–1138, 1998.

[2] D. Johnston, "TM4 motor-wheel drive and control system: Performance, benefits and advantages," in *CD-ROM Proc. EVS-17*, 2000.

[3] Yasuji Shibahata et al., "The improvement of vehicle maneuverability by direct yaw moment control," in *Proc. AVEC '92*, 1992, number 923081.

[4] Sumio Motoyama et al., "Effect of traction force distribution control on vehicle dynamics," in *Proc. AVEC '92*, 1992, number 923080.

[5] Shin-ichiro Sakai, Hideo Sado, and Yoichi. Hori, "Novel skid avoidance method without vehicle chassis speed for electric vehicle," in *Proc. International Power Electronics Conference (IPEC)*, Tokyo, Japan, 2000, vol. 4, pp. 1979–1984.

[6] Shin-ichiro Sakai, "Project of motion control in an electric vehicle with four in-wheel motors," URL: http://www.hori.t.u-tokyo.ac.jp/997/sakai/Research/index.html, 1999.

[7] Shin-ichiro Sakai and Yoichi. Hori, "Advanced vehicle motion control of electric vehicle based on the fast motor torque response," in *Proc. 5th International Symposium on Advanced Vehicle Control (AVEC)*, Michigan, USA, 2000, pp. 729–736.

[8] Y. Furukawa and M. Abe, "Direct yaw moment control with estimating side-slip angle by using on-board-tire-model," in *Proc. 4th International Symposium on Advanced Vehicle Control*, Nagoya, 1998, pp. 431–436.

[9] Masato Abe, Yoshio Kano, and Kazuasa Suzuki, "An experimental validation of side-slip control to compensate vehicle lateral dynamics for a loss of stability due to nonlinear tire characteristics," in *Proc. AVEC 2000*, 2000, pp. 179–186.

Affiliation

Shin-ichiro Sakai, Ph.D. / The Institute of Space and Astronautical Science
3-1-1, Yoshinodai, Sagamihara, Kanagawa, Japan;
Phone: +81-42-759-8308, Fax: +81-42-759-8473
E-mail : sakai@pub.isas.ac.jp, URL: sakai.nnl.isas.ac.jp/index.html

He received the Ph.D. degrees in electrical engineering from the University of Tokyo in 2000. He worked as JSPS Research Fellow in the University of Tokyo in 2000, and since 2001 he has been a research associate in The Institute of Space and Astronautical Science.

Yoich Hori, Ph.D. / The University of Tokyo
7-3-1 Hongo, Bunkyo Tokyo 113-8656, Japan;
Phone: +81-3-5841-6678, Fax: +81-3-5841-8573,
E-mail : hori@hori.t.u-tokyo.ac.jp, URL: www.hori.t.u-tokyo.ac.jp

He received the Ph.D. degrees in electrical engineering from the University of Tokyo in 1983. He joined the Dept. of Elec. Eng. at the Univ. of Tokyo as a research associate in 1983. Since 2000, he has been a professor.